Study of the Hydrogen, Helium, and Heavy Nuclei in the November 12, 1960 Solar Cosmic-Ray Event

S. BISWAS*, C. E. FICHTEL, AND D. E. GUSS

*Goddard Space Flight Center, National Aeronautics and Space Administration,
Greenbelt, Maryland*

(Received May 4, 1962)

A study of the composition and energy spectra of solar cosmic rays from the Nov. 12, 1960 solar flare has been made using rocket-borne nuclear emulsions. The abundances of hydrogen, helium, carbon, nitrogen, oxygen, neon, and larger nuclei have been determined, and upper limits were set for light nuclei ($3 \leq Z \leq 5$) and fluorine nuclei. The relative numbers of helium, light, medium ($6 \leq Z \leq 9$), and large ($Z \geq 10$) nuclei in the solar beam were found to be 680 ± 110, <0.1, 10, and 1.0 ± 0.3, respectively. The composition was seen to be similar to that of the solar atmosphere as determined by spectroscopic means, for those elements where a comparison could be made, but markedly different from that of galactic cosmic rays. The differential energy per nucleon spectra of hydrogen, helium, and medium nuclei could be represented by an equation of the form $dJ/dW = K(W/W_0)^{-\gamma}$ for kinetic energies greater than 35 MeV per nucleon. The values of γ for He nuclei and medium nuclei were the same within uncertainties, but were larger than that for hydrogen nuclei by a factor of more than two in the energy interval from 40 to 130 MeV/nucleon. In spite of the different energy/nucleon spectra, the ratio of protons to heavier nuclei in the same energy/nucleon interval was the same at different times in the event and also the same as that observed in two other events. The measurements are shown to be consistent with a diffusion process which has a predominantly velocity dependent diffusion coefficient at low energies, as suggested by Parker, and therefore the different energy/nucleon spectra mentioned earlier are most probably due to differences generated by the acceleration process. Present ideas concerning the acceleration mechanism for solar cosmic rays are discussed in relation to the experimental results.

I. INTRODUCTION

MANY studies have been made of the proton energy spectrum of solar cosmic-ray events using balloons and satellites. Information on the helium nuclei at balloon altitudes[1,2] has been obtained in several events by the University of Minnesota's nuclear emulsion group. In a NASA sounding rocket firing which was a part of the solar cosmic-ray experiment at Fort Churchill, Canada, we previously obtained some information on the protons, helium nuclei, and heavy nuclei ($Z \gtrsim 3$) at one time during the Sept. 3, 1960 event.[3] Although these results gave the first indication of the very gross relative abundances of the heavy nuclei and the heavy to proton ratio, the very limited statistics did not permit a detailed analysis of the composition or a determination of the energy spectrum of any but the proton component.

Subsequently, two similar rocket firings with successful nuclear emulsion recovery were made during the high intensity Nov. 12, 1960 solar cosmic-ray event in which it was discovered that there were sufficient numbers of particles to permit a detailed analysis on the helium and heavy nuclei. This paper is devoted to an analysis of the particle properties of the Nov. 12, 1960 event as determined from the nuclear emulsions recovered from the two firings just mentioned. In particular, the charge composition is studied up to charge eighteen for particles with an energy per nucleon in excess of a few tens of MeV. A comparison of the energy spectra of the protons, helium nuclei, and medium nuclei ($6 \leq Z \leq 9$) in the same energy intervals and the same rigidity intervals is made. This new information is then discussed in terms of some of the existing theoretical models related to solar cosmic-ray events in an attempt to obtain a better understanding of the sun, the acceleration mechanism for these high-energy particles, and the interplanetary modulation. Finally, the composition of the solar cosmic rays is compared to that of ordinary galactic cosmic rays to show that there are some very marked differences.

II. DESCRIPTION OF THE EVENT

The Nov. 12, 1960 event was one of the largest ever recorded. The total integrated particle flux for this event is estimated to be about 2×10^8 particles/(cm^2 sr) for particles with energies greater than 20 MeV. This is almost two orders of magnitude greater than the normal galactic cosmic-ray flux for a whole year. Further, the integral energy flux was approximately 3×10^4 ergs/(cm^2 sr), which is somewhat larger than that from cosmic rays for a year.

The flare considered to be the source of the solar cosmic-ray particles which began to reach the earth on Nov. 12, 1960 was preceded by a period of relatively important solar activity. On Nov. 10, 1960, there was a class 3 flare at 1000 U.T. in the McMath plage region 5925. A major type IV radio noise outburst was observed in Japan and Australia beginning at about 0304 U.T. Nov. 11, 1960. At approximately the same time, Voroshilov observed a major flare which reached a maximum at about 0340 U.T. At 1322 U.T. on Nov. 12, 1960, a class 3 flare occurred, and very shortly thereafter at 1340 U.T. a neutron monitor increase began at Deep

---

* NASA-National Academy of Sciences Postdoctoral Resident Research Associate; on leave from Tata Institute of Fundamental Research, Bombay, India.

[1] S. Biswas, P. S. Freier, and W. Stein, J. Geophys. Research **67**, 13 (1962).

[2] E. P. Ney and W. Stein, J. Phys. Soc. Japan **17**, Suppl. A-II, 345 (1962).

[3] C. E. Fichtel and D. E. Guss, Phys. Rev. Letters **6**, 495 (1961).

River[4] and other stations. Two magnetic storms followed shortly at 1348 and 1844 U.T. They are believed to be associated with the major flares on Nov. 10 and 11. Following the second sudden commencement, at 1900 U.T. there was a second sharp increase in the Deep River neutron monitor counting rate which, after having increased for $2\frac{1}{2}$ h, had begun to decline. However, at the same time there was a Forbush decrease on the MIT meson telescope, indicating the very high-energy galactic cosmic rays were being partially excluded from the region of the earth.

Vogan and Hartz[5] observed that the 60-Mc/sec riometers showed a sharp increase in absorption at approximately 1900 U.T. on Nov. 12, 1960. Steljes et al.[4] have shown that these and other considerations form a solid base for the proposition that the particles from the 1322 U.T. Nov. 12 flare were at least partially contained within the walls of a "magnetic bottle" formed by the gas cloud associated with the Nov. 11 flare expanding from the sun. There was a considerable leakage from the bottle as indicated by the increase in particle intensity prior to 1900 U.T. Nov. 12. The first of the two recovered payloads was fired at 1840 U.T., and, therefore, the information gathered represents a sample of the particle flux just before the effects of the second magnetic storm were felt.

At 1021 U.T. on Nov. 13, 1960, there was another sudden commencement, presumably associated with the Nov. 12 flare, followed by another Forbush decrease at 1035 U.T.[4] No appreciable prolonged change was noted in the riometer absorption at this time indicating this second sudden commencement had little effect on at least the low-energy component, which, according to the riometer, was only slightly less than maximum intensity. The second firing from which a payload was recovered occurred at 1603 U.T. on Nov. 13, 1960, and, therefore, represents a study of this period of near maximum low-energy flux.

After this time, the particle density, as measured by the riometer and balloon flights at Minnesota, continued to decrease until early on Nov. 15, when another solar cosmic-ray event began, and prevented the further study of this event.

A summary of the Deep River neutron monitor record,[4] the Fort Churchill riometer data,[6] and our flight times are shown in Fig. 1.

III. EXPERIMENTAL PROCEDURE

A. Rocket and Payload System

In order to study the low-energy component of solar cosmic rays and to take advantage of the special properties of nuclear emulsions to examine their charge spec-
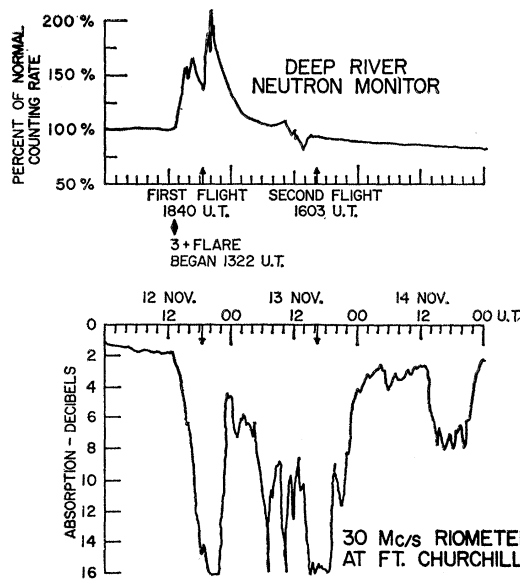

FIG. 1. Deep River neutron monitor record and the Fort Churchill riometer absorption curve, Flight times for the rockets of this experiment are indicated by arrows.

trum, research sounding rockets with recoverable payloads were kept on a 24 h per day standby at Fort Churchill, Canada, from June 6, 1960, until the end of the firings in Nov. 1960. The Nike-Cajun rocket was chosen because: It could be prepared for firing quickly; a number could be kept on standby for launching into the same event; it could carry the 85-lb payload to a peak altitude of 130 km, permitting a several minute exposure under less than 0.01 g/cm² of atmosphere; a recovery system existed for the Nike-Cajun which could be easily modified for our needs; it could be fired from Fort Churchill, where the entry of the low-energy particles to be studied is not prevented by the earth's magnetic field;[7-9] and it was a proved system.

The payload[10] itself was divided into four parts, a recovery section, a nuclear emulsion section, an instrumentation section, and an ogive nose cone. The recovery section included a parachute, a SARAH beacon, dive brakes for reentry stabilization, and dye packages. The sequence of operation of the recovery section is illustrated along with the Nike-Cajun trajectory in Fig. 2. Successful recovery of the payload depended primarily on homing in on the SARAH beacon with a helicopter, impact prediction by SOTIM[11], and visual sighting, since attempts to track the rocket flights by

[4] J. F. Steljes, H. Carmichael, and K. G. McCracken, J. Geophys. Research 66, 1363 (1961).

[5] E. L. Vogan and T. R. Hartz, Can. J. Phys. 39, 630 (1961).

[6] Courtesy of Defense Research Telecommunications Establishment, Ottawa, Canada.

[7] J. J. Quenby and W. R. Webber, Phil. Mag. 4, 90 (1959).

[8] P. Rothwell, J. Geophys. Research 64, 2026 (1959).

[9] L. L. Cogger, Chalk River Laboratory Report CRGP-965, 1960 (unpublished).

[10] The payload was constructed by Cook Research Laboratories in accordance with the specifications of the Goddard Space Flight Center.

[11] A system whereby several sets of microphones on the ground are used to receive the sound produced by reentry of the payload into the atmosphere. An impact point is estimated by triangulation.
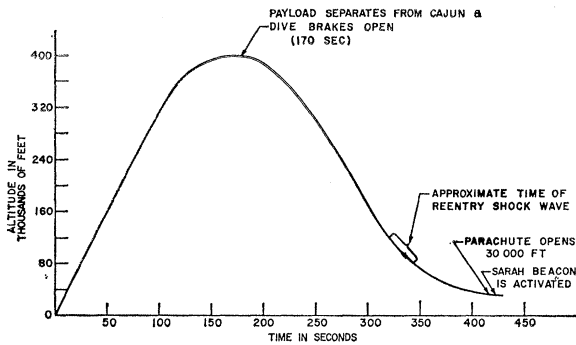
FIG. 2. Nike-Cajun trajectory.

radar failed. In spite of difficult recovery conditions, two of the three payloads fired into the Nov. 12, 1960 event were recovered.

The nuclear emulsion section consisted of a central cylinder of forty 600 μ thick Ilford G5 nuclear emulsions in the shape of 4-in.-diam disks whose planes were perpendicular to the rocket axis, four structural posts 90° apart, and an outside cylindrical aluminum skin which was $6\frac{3}{4}$ in. in diameter and 0.024 in. thick. This thickness was the minimum which would withstand the heat and strains of the flight and still maintain a water-tight seal. As an additional protection against heat, the emulsions were covered with thin heat radiation reflecting aluminum foil. A sheet of 1-mil Mylar was placed between the foil and the emulsions to prevent the aluminum from reacting with the emulsions. The total amount of material between the emulsions and the ambient radiation, once the payload was out of the atmosphere, was then 0.19 g/cm², largely aluminum.

The instrumentation section contained flight performance instruments, including a magnetometer and accelerometer, and electronic counters, the data from which are being published separately.[12]

B. Proton Component

The emulsions were scanned on specially constructed microscope stages which provided precision rotational motion about the center of the circular emulsion sheet and a radial motion. The scanning was performed in the middle 80% of the emulsion thickness at distances of 0.5 mm, 1.3 mm, and 3.5 mm in from the edge for all tracks lying in the solid angle interval defined by $|\alpha| \leqslant 20°$ and $|\beta| \leqslant 20°$, and at distances 10.00 mm and 20.0 mm for all tracks in the solid angle interval defined by $|\alpha| \leqslant 20°$ and $|\beta| \leqslant 10°$. Here α is the angle between the projection of the track on the plane of the emulsion and the radius vector of the emulsion disk measured at the scan line, and β is the angle of the track with respect to the plane of the emulsion. The usual scanning efficiency checks,[13] such as comparing the distributions

of number of tracks found versus α, β, and emulsion depth with the expected distributions and rescanning by a second scanner, were performed. In addition, scans were performed in all four quadrants of the emulsion disks and the intensity of tracks obtained in each was found to be the same within the statistical uncertainties. This would be expected, since the rocket was known to be spinning rapidly about its axis during the flight.

The scans described above make it possible to derive integral proton intensities in the range of energies between 14.5 and 81 MeV. To extend the spectrum to higher energies, the energies of those particles producing tracks in the scan 10.00 mm in from the edge of the emulsion were determined from ionization measurements, using the Fowler-Perkins method[14] of the blob-gap counting. The tracks were selected for the blob-gap measurement, if they had an ionization greater than 1.3 times minimum as determined from a prior blob count. This was two standard deviations below the ionization corresponding to the highest energy point included in the integral spectrum. Because the spectrum is a steeply falling function of energy in this energy region, the finite resolution of the ionization measurements results in an artificial increase of particles toward higher energy, and a shift of the order of 4% was made to compensate for this effect.

The results obtained from the scans described above must be corrected for particles other than solar protons which are picked up in the scans. These are background tracks collected before and following the flight, galactic cosmic-ray protons collected during the flight, and solar He nuclei. Because of the shape of the energy spectrum, the contribution of secondary tracks from interactions in the emulsion is negligible for the range of energies under discussion. The contribution from background tracks was determined from scans in emulsions which were kept with the flight stack at all times except during the rocket flight, and the contribution from galactic cosmic-ray particles was determined from scans in the emulsion stack which was flown during a solar "quiet" time. The correction to the particle densities from both of these contributions was less than 1% at proton energies less than 120 MeV. At higher energies these corrections became appreciable, and the high energy limit of the spectrum was set at that energy where the expected background contribution was the same order as the sample; 340 MeV in the first flight and 270 MeV in the second. The contribution of solar He nuclei was determined as described in the next section, and this correction was made to the proton flux.

In order to calculate intensities, some assumption must be made about the isotropy of the solar particles. It was assumed that the solar particles during these flights were isotropic over zenith angles $\theta \leqslant 90°$ and zero for zenith angles $\theta \geqslant 90° + \delta$. The particles which are

[12] K. Ogilvie, D. Bryant, and L. Davis, J. Geophys. Research 67, 929 (1962).
[13] C. E. Fichtel, Nuovo cimento 19, 1100 (1961).

[14] P. H. Fowler and D. H. Perkins, Phil. Mag. 46, 587 (1955).

present between 90° and 90°+δ are those which have mirrored in the magnetic field of the earth below the altitude of the rocket and returned. The mirrored particles are degraded in energy by ionization loss in the atmosphere while twice traversing the spiral path from the rocket altitude to the mirror point. The angle δ is a function of the ambient proton energy and the rocket altitude; however, even for the highest energy particles considered, δ did not exceed 10°. An analysis of the Geiger counter data on the flights is consistent with these assumptions.[12]

With the above assumption of isotropy, an integral energy spectrum can be constructed from the data which has been corrected for background, galactic cosmic rays, and solar He nuclei. This spectrum is a good first approximation to the ambient spectrum, and using it as a trial spectrum, the true spectrum of solar protons, corrected for rocket trajectory, is obtained by a method of iteration as explained below.

The trajectory correction consists of two parts: (1) those particles which are collected by the emulsion in its ascent and descent through the atmosphere, and (2) those particles which are collected when the rocket is above the atmosphere. The particles in (1) are degraded in energy by ionization loss in the atmosphere above the dectector: Those in (2), which arrive from zenith angles greater than 90°, are also degraded in energy by ionization loss in the atmosphere between the rocket altitude and the mirror point. The remainder of the particles, those collected in the upper hemisphere when the rocket is above the atmosphere, and comprising more than 80% of the particles collected, are at the original energy.

The shape of the trial spectrum after passing through various amounts of atmosphere was constructed from range energy tables.[15] In principle, the total contribution to the particle density for the trial function can then be calculated by integrating the appropriate energy spectrum at a given point and angle over the entire solid angle of acceptance and collecting area for the known orientation of the payload at each point on the trajectory, and then integrating over the entire flight. In practice these integrals were approximated by summations. To this sum was added a small contribution for penetration, i.e., those particles which crossed the scan line from below, having first traversed the emulsion stack. The absorption length and shift in the energy spectrum resulting from interactions of protons in emulsion are not known well. It was assumed here that an interaction of a proton produced one proton of approximately the same energy and direction, and the contribution from penetration was determined by constructing the shape of the trial spectrum at an absorber depth equal to the amount of atmosphere and emulsion traversed. As seen in Table I, the con-

[15] J. H. Atkinson, Jr. and B. H. Willis, University of California Radiation Laboratory Report UCRL-2426 (rev)-II (unpublished).

TABLE I. Fractional contribution to observed integral proton intensity from various absorber depths.

Energy E (MeV)	g/cm² of atmosphere							"Penetration"
	0–0.2	0.2–0.7	0.7–1.5	1.5–6	6–15	15–25	25–35	
15	0.88	0.04	0.03	0.02	0.01	0	0	0.02
20.5	0.86	0.05	0.03	0.02	0.01	0	0	0.03
31	0.82	0.05	0.04	0.03	0.01	0	0	0.05
56	0.76	0.05	0.04	0.04	0.02	0.01	0	0.08
81	0.75	0.05	0.04	0.04	0.02	0.01	0	0.09
120	0.70	0.05	0.05	0.04	0.02	0.01	0	0.13
160	0.66	0.05	0.05	0 05	0.02	0.01	0	0.16
220	0.62	0.05	0.04	0.04	0.03	0.01	0	0.21
270	0.62	0.04	0.04	0.03	0.03	0.01	0	0.23

tribution resulting from penetration varied from 2 to 23% of the sample. The systematic error resulting from this procedure was included in the systematic error resulting from the trajectory correction. It should be noted that the contribution from penetration is small, and that it is largest at high energies, where the statistical error rather than the systematic error governs the total error.

The particle density in units of particles/cm² sr obtained from the procedure outlined above was then compared to the observed particle density. On the basis of this comparison, a better estimate of the primary spectrum was made and the procedure repeated until the trial spectrum produced the observed particle densities. In both flights the second trial spectrum fitted the observed data.

Table I shows the contribution to the observed integral intensity which was obtained under various absorber thicknesses for the flight at 1840 U.T. on Nov. 12 and is typical of all of the rocket flights. The energy E in the table is the energy calculated assuming no absorber was above the emulsion except the wrapping and rocket skin. It can be seen from the table that from 62 to 88% of the sample, depending on energy, was obtained at zero atmosphere. The error arising from this procedure is estimated to be essentially zero for that portion of the particles collected above the atmosphere and no more than 30% for that portion of the sample collected under some residual atmosphere. The estimated error from this source then depends on energy and is of the order of 6% for the lower energies (≤ 81 MeV). The combined error introduced by the uncertainty in measurements of the solid angle of acceptance and the collecting area is 5%. Combining this error with the other uncertainties mentioned above one obtains a root mean square error of about 8% at low energies and a somewhat larger value of 10–15% at high energies (120–270 MeV). This systematic error was combined with the statistical uncertainty to yield the errors listed in Table III.

C. Helium Component

In order to obtain the flux and energy spectra of the helium nuclei in the solar particles, the emulsions flown in the first flight were scanned along a line at a distance

of 5 mm from the edge of the emulsion. All particle tracks crossing this scan line in the middle half of the emulsion thickness were recorded if they had nine times minimum ionization or greater, and were within a solid angle defined by $|\beta| \leqslant 3.5°$ and $|\alpha| \leqslant 45°$. With these criteria, the ambient energy interval was 37.5 to 180 MeV/nucleon. The particle tracks were followed through the emulsion stack until they came to rest or interacted. Grain density and delta-ray[16] density measurements as a function of residual range were made on about 1200 tracks to resolve He nuclei from protons. The helium tracks, of which there were 50, were followed from the scan to the outer edge of the emulsion and those originating from interactions in the emulsion above the scan line were rejected. The very small correction for loss of He nuclei due to interactions in the emulsion and the shielding was made assuming an interaction length of 20 cm in emulsion. The ambient energy of the particles was obtained from range measurements except for one particle which interacted in the emulsion. Its energy was determined from a multiple scattering measurement. The scanning efficiency for the detection of helium nuclei was found to be essentially 100%.

A similar procedure was followed for obtaining helium nuclei in the second flight. In this case the scan line was 3 mm from the edge, and all particles having an ionization of $\geqslant 11.0$ times minimum, $|\beta| \leqslant 5.5°$, and $|\alpha| \leqslant 45°$ were recorded. From 1350 particle tracks, 70 helium nuclei were obtained having ambient energies between 29 and 130 MeV/nucleon.

In order to calculate the flux and energy spectra of the helium nuclei in free space, the effective time and solid angle are calculated in a manner similar to that for the protons.

D. Deuterons and Tritons

In the course of the analysis of the solar helium nuclei in the first flight, an arbitrary sample of 300 tracks was examined for the presence of deuterons and tritons. The particle tracks scanned and selected for measurements belonged to the following ambient energy intervals: protons, 40 to 56 MeV; deuterons, 50 to 95 MeV; and tritons, 60 to 130 MeV. Integral delta-ray counts were made over the last two millimeters of range. From a plot of the frequency distribution of delta rays, about 100 tracks were selected which would contain 80% of the deuterons and tritons present in the entire sample of 300 tracks. Accurate ionization and range measurements were made on these tracks to resolve protons, deuterons, and tritons.

E. Heavy Nuclei

In order to determine the characteristics of the heavy nuclei in the solar cosmic-ray event, a complete scan of
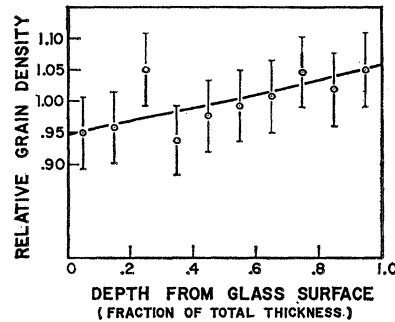

FIG. 3. The variation of grain density with depth in emulsion as obtained from measurements on tracks of fast particles.

the periphery of the nuclear emulsion disks, 0.7 mm from the edge was made for tracks of heavy nuclei within a solid angle, $|\beta| \leqslant 20°$ and $|\alpha| \leqslant 45°$. The scanning efficiency safeguards and checks, including additional scanning further in from the edge of the plates than the original scan (at 2.5 mm and 6.5 mm from the edge) were similar to those used for the proton component. There was no indication of particles being missed.

After elimination of the tracks which could be identified as having been formed by helium nuclei, measurements were made on the remainder to determine the charge and energy of the primary nucleus which produced the track. For this purpose, it was sufficient to record the range of the particle and its relative rate of energy loss. The very small number of the heavy tracks which had sufficiently high energies so that they did not come to rest in the stack was found to be consistent with that expected from the normal high-energy galactic cosmic-ray flux. Therefore, the range could be used as one parameter for the solar heavy nuclei. The range of a heavy nucleus, $R_{(H)}$, is given by the expression[17]

$$R_{(H)} = (M/Z^2)R_{(proton)} + R_{(ext)}, \tag{1}$$

where $R_{(ext)}$ is a very small term. Since $R_{(proton)}$ is a function of v/c and known constants, and $R_{(ext)}$ is known, Eq. (1) gives $R_{(H)}$ in terms of Z and v/c.

In order to determine the relative rate of energy loss, the delta-ray density method was used since it gave a more reliable estimate of the charge than the thin down or effective track width measurements. Both the four grain delta-ray density criteria and the method of counting delta rays whose projected length in the plane of the emulsion extended beyond two parallel lines at a fixed distance on each side of the primary track were tried. The resolution obtained by the two methods was similar, with the latter being slightly better. In order to provide an adequate length for charge resolution measurements, a range of at least one millimeter in the emulsions was demanded for all tracks included in the final analysis. This restriction, plus the material between the emulsion and the ambient radiation, set the lower limit on the energy.

---

[16] A "delta ray" is a secondary electron track, originating from the primary track.

[17] H. H. Heckman, B. L. Perkins, W. G. Simon, F. M. Smith, and W. H. Barkas, Phys. Rev. **117**, 544 (1960).

Since the delta-ray density varies with the degree of development, the matter of variations in development must be considered. In general, it was felt to be better to try to avoid variations rather than to have to correct for them; and this was done whenever possible. Therefore, the delta-ray density over a given length was measured rather than the integral number of delta rays from the end of the track, since in this way it was usually possible to avoid most of the nonuniformities now to be discussed and still lose relatively little in resolution due to slightly reduced statistics. Since a large number of acceptable heavy nuclei tracks were found in each plate, about fifty in the first flight and eighty in the second, a self-consistent charge calibration was possible for each plate; thereby circumventing the problem of emulsion to emulsion development variations. For a small portion of the tracks, it was necessary to make a count in two plates to obtain the desired statistics; in these cases a statistically weighted average of the Z determination was used as the final value. The emulsion to emulsion variations in delta-ray density was $\lesssim 3\%$ in these plates.

There are also several kinds of sensitivity variations which can occur within an emulsion plate. Nonuniformity with depth can now usually be largely avoided by use of known developing procedures. The variation of grain density with depth for a plate from the first flight is shown in Fig. 3, for example. In addition, delta-ray measurements were not made in the top or bottom 15 μ in any case, and were made in the top or bottom 45 μ for only approximately 10% of the tracks where a meaningful measurement could not be made on the track without doing so. The counting was performed at the same distance in from the edge whenever possible and the small correction for average development over the length of the count was made for the few cases where this was not possible. Figure 4 shows the variation of grain density with distances in from the plate edge. The plates were further examined for local nonuniformities. For the relationship between delta-ray variations with grain density variations, it was necessary to use high-energy heavy tracks of the appropriate delta-ray density in cosmic-ray plates developed to a similar degree and with similar grain
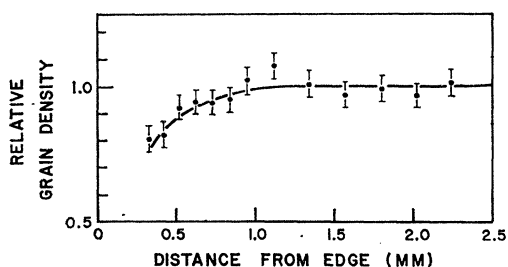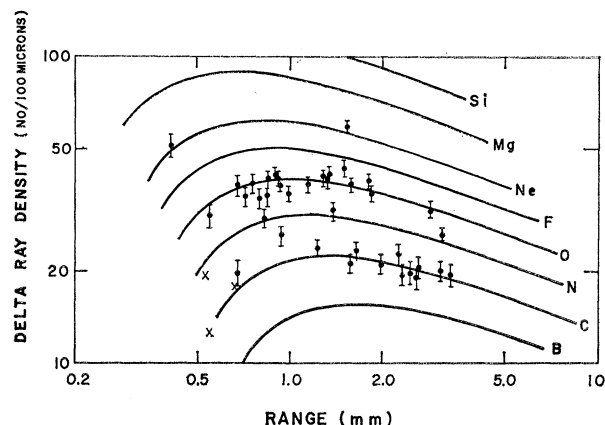

FIG. 5. Plot of delta-ray density as a function of range for measurements made within a single plate. A few tracks for which N_δ exceeded 100/100 μ are not shown, as well as one for which the range exceeded ten millimeters. The length of the vertical line associated with each point gives the uncertainty due to the number of delta rays counted only. The small corrections for development variation have been made for the cases where it was not negligible, as explained in the text. Points marked with a cross were not included in the final results because, although they satisfied the range criteria, they correspond to particles whose energies were below the cutoff limit.

size since no tracks of this type were found in the short solar particle exposure. However, since the correlation should be nearly the same and since the correction for sensitivity gradients was usually small compared to the statistical uncertainty, 2 to 3% on the average compared to 6 to 10%, no significant error should be introduced by this procedure.

The general subject of delta-ray counting, the associated uncertainties, and statistical errors is a complex one, which, however, has been treated extensively[13,18,19] and, therefore, only a few more remarks will be added. For consistency on the part of the observer, it is advisable to recount standard tracks of various delta-ray densities frequently and this was done. The constant correction for background electrons is very small compared to the delta-ray densities measured in the region of interest, approximately 1% of the plateau value for oxygen.

The variation of the delta-ray density with v/c as measured by the second delta-ray-density method, namely, counting those secondary electrons whose projected length in the plane of the emulsion extend beyond some fixed distance was found to agree well with Mott's formula, which also has been shown previously to be a good representation of the experimentally observed distribution.[18,19] The correction for the difference between the average of the delta-ray density measured over a finite length and the theoretical value at the midpoint was made with the use of this formula. Again the correction is small compared to the statistical

FIG. 4. The variation of grain density as a function of the distance from the edge of emulsion as obtained from tracks of fast particles.

[18] H. Aizu, Y. Fujimoto, S. Hasegawa, M. Koshiba, I. Mito, J. Nishimura, K. Yokoi, and M. Schein, Phys. Rev. 116, 436 (1959).
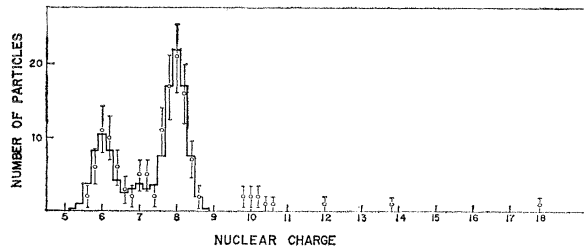[19] E. Tamai, Phys. Rev. 117, 1345 (1960).

FIG. 6. The charge distribution for heavy nuclei from the flight at 1840 U.T. on Nov. 12. The experimental points are marked by open circles. The expected distribution for a root mean square uncertainty of 0.27 of one charge for medium group of nuclei, is shown by the solid histogram assuming the relative abundances of B, C, N, O, and F nuclei to be 0, 5, 1.7, 10, and 0, respectively.

uncertainty. There is no simple model giving the variation of the four grain delta-ray density with range because the variation in track width with range causes the cutoff energy corresponding to a delta ray with four observable grains to change. Experimental curves can be developed and were obtained. However, as mentioned earlier, the former method gave better resolution; so those results are presented and are shown in Fig. 5.

By a method described in detail in a previous paper,[13] the charge resolution obtained experimentally for the medium nuclei was found to be 0.27 of a charge. This is about the same as the average root mean square uncertainty for charge determination in this charge group as expected from statistical uncertainty. For nuclei with charges of ten or more the accuracy begins to decrease slowly with charge. A correction was made to the nitrogen abundance for the effect of the addition of particles from the tails of the carbon and oxygen components in the manner outlined in the above-mentioned reference. However, since the correction is significant, it is perhaps best to regard the nitrogen abundance as an approximate upper limit. The limits set for the fluorine and boron components are due primarily to the oxygen and carbon tails, respectively. A diagram showing the charge resolution for tracks from the first flight is shown in Fig. 6; the resolution for the other flight was similar. In addition to the experimental points, indicated by open circles, the expected distribution for a root mean square uncertainty of 0.27 of one charge is shown, assuming the relative abundances of B, C, N, O, and F to be 0, 5, 1.7, 10, and 0, respectively.

For comparison, we have shown in Fig. 7 the expected histogram for a composition similar to that of galactic cosmic radiation for the same charge resolution. For this histogram, the relative abundances of B, C, N, O, and F were taken to be 1, 2, 1, 1.3, and 0, respectively. The number of particles obtained for each interval in such a diagram is usually of the order of 5. Thus, it is seen that, except for carbon, the distribution shows less pronounced peaks than is the case for the solar particles, especially if there are a few large fluctuations. A typical distribution of this type is shown in reference 18. In

TABLE II. Fractional contribution to observed integral medium nuclei intensity from various absorber depths.

Kinetic energy per nucleon (MeV)	g/cm² of atmosphere				
	0-0.2	0.2-0.7	0.7-1.5	1.5-6	>6
42.5	0.96	0.03	0.01	≅0.002	0
54.9	0.95	0.03	0.02	≅0.003	0
68.8	0.94	0.03	0.02	≅0.005	0
95	0.92	0.04	0.03	0.01	≅0.005

that experiment, the expected error is similar to this experiment due to the fact that, though the statistical error is somewhat less by a factor of about 0.75, the problem of plate-to-plate normalization necessitated by the low galactic heavy flux approximately compensates for this effect. The degree of resolution in the present experiment may also be helped somewhat by the particularly favorable development of this set of plates.

It is seen then that the resolution would be expected to be similar to ordinary cosmic-ray studies, as it is, and what appears to be a sharper resolution when a first look is taken at Fig. 6 is in reality only a reflection of the different composition of the two types of radiation.

The only subject related to the charge measurements which is still to be discussed is the matter of absolute charge calibration. The particular difficulty was the complete absence of low-energy light nuclei (Li, Be, and B), which meant there was a gap of several charges between helium nuclei and the higher charges. The expected normalizing constant for the curve of the delta-ray density, N_δ, as a function of range, R, was obtained in two ways; first from the tracks of carbon and oxygen nuclei in normal cosmic-ray balloon flight nuclear emulsion plates developed to the same degree, and secondly, and with less certainty, from the helium nuclei curve in these plates. Whereas the latter method was used only as a check, the former method should lead to an error of no more than two-tenths of one charge. In fact, the experimental points predominately clustered around the expected curves for carbon and
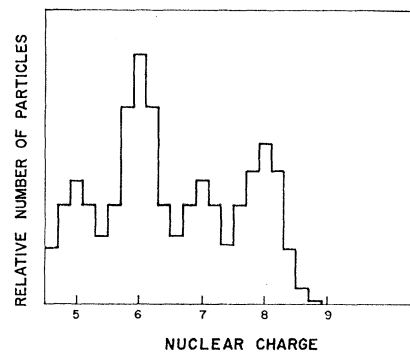

FIG. 7. The calculated charge distribution for a composition similar to that of galactic cosmic radiation assuming the same charge resolution as shown in Fig. 6. The relative abundances of B, C, N, O, and F nuclei were assumed to be 1, 2, 1, 1.3, and 0, respectively.

TABLE III. Integral and differential flux values for protons.

Kinetic energy (MeV)	Flux at 1840 U.T. Nov. 12, 1960	Flux at 1603 U.T. Nov. 13, 1960
	(a) Integral Flux Values	
	(part./cm² sr sec)	(part./cm² sr sec)
15	1690 ±190	5160 ±520
20.5	1290 ±140	3690 ±370
31.3	850 ± 94	2180 ±240
56	501 ± 55	842 ± 81
81	310 ± 34	350 ± 39
120	127 ± 15	78 ± 9
160	69 ± 10.4	27 ± 4
220	24.3± 5.4	6.6± 1.3
270	8 ± 3.0	
	(b) Differential Flux Values	
	(part./cm² sr sec MeV)	(part./cm² sr sec MeV)
17.5	73 ±24	267 ±72
25.5	40.7 ±12	140 ±26
43	14.1 ± 3.5	54 ± 8
68	7.6 ± 1.9	19.7 ± 3.1
100	4.7 ± 1.1	7.0 ± 0.9
138	1.45± 0.35	1.3 ± 0.2
186	0.74± 0.18	0.34± 0.06
243	0.33± 0.12	0.08± 0.03
306	0.10± 0.04	

oxygen so well that the final best curves, based on assuming the tracks to be formed by these nuclei, differed from the expected curves by less than one-tenth of a charge.

In order to calculate the flux and energy spectra of the heavy nuclei in free space, a procedure essentially identical to that for the proton component was used. As shown in Table II, the contribution during the ascent and descent phase is seen to be smaller than for the protons both because of the steeper energy spectrum and the higher rate of energy loss per nucleon. Again because of the wall and the minimum track length accepted for analysis, there was always about 0.61 gm/cm² of material in the payload for any acceptable particle to go through. Therefore, the cutoff energy remained essentially constant for most of the effective collecting time and solid angle. For a similar reason, the effective collection times for the heaviest nuclei which were accepted were nearly the same as those of the medium nuclei. although the minimum energy per nucleon, determined by the minimum accepted range, increased with charge.

IV. RESULTS

A. Singly Charged Particles

From the measurements described in Sec. IIIA, the integral and differential energy spectra of solar protons in the kinetic energy interval from 14.5 to a few hundred MeV were obtained. The flux values measured in the two rocket flights are given in Table III. The integral flux above 340 MeV in the first flight and 270 MeV in the second was estimated by extrapolating the differential energy spectra. These values are such that the
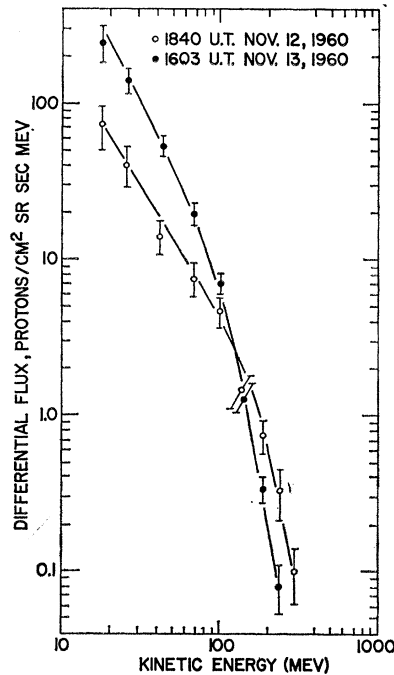

FIG. 8. Differential kinetic energy spectra of protons during the two flights.

uncertainty introduced into the integral flux values is negligible except for the highest energy points quoted.

The errors shown in the integral flux values included both the statistical and systematic errors which enter in the measurements. In the integral flux values the statistical errors are 6% in the energy interval from 14 to 81 MeV and then gradually increase from 6 to 25% in the energy interval from 120 to 340 MeV. Systematic uncertainty is given in Sec. IIIB. The differential flux was calculated from the integral flux values. The error was obtained by calculating the statistical error as that arising from the statistical errors of the two integral points and combining this error with the systematic uncertainty to obtain the total error.

The differential energy spectra of solar protons in the two rocket flights shown in Fig. 8 indicate that very significant changes occurred. In the second flight the intensity of low-energy protons had increased while that of high-energy protons had decreased as compared to those in the first flight.

The proton spectrum at any time cannot be represented by a power law spectrum of the form

$$dN/dE = KE^{-n}, \qquad (2)$$

where E is the proton kinetic energy in MeV, and K and n are constants. Consider, for example, the first flight, where

$$d[\ln(dN/dE)]/d[\ln E]$$

varies from about 1.5 in the energy interval from 15 to 40 MeV to a value of about 5 in the energy interval
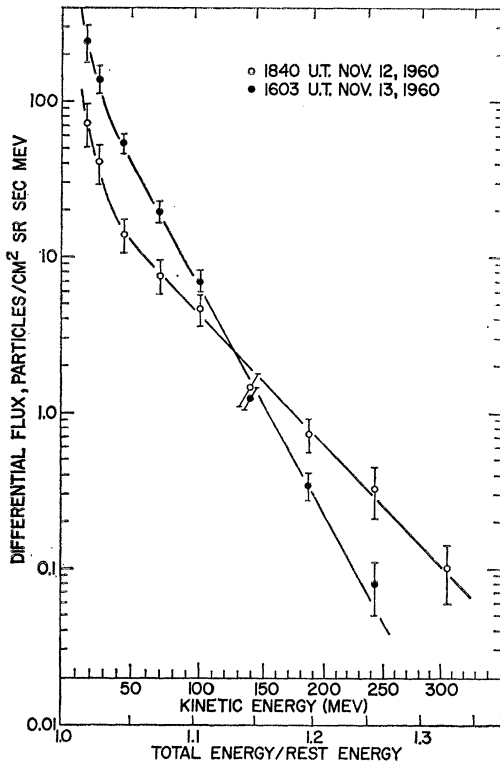
FIG. 9. Differential proton flux as a function of total energy in units of the rest energy. Note that the abscissa is an expanded logarithmic scale.

from 200 to 300 MeV. In the second flight, the spectrum behaves in a similar manner. This feature was even more pronounced in the results obtained during the Sept. 3, 1960 flare event.[20]

An alternative way of expressing the proton energy spectrum is as a power law of the total energy.

$$\frac{dN}{dE}=C/(1+E/W_0)^\gamma=\frac{C}{(W/W_0)^\gamma}, \tag{3}$$

where W is the total energy and W_0 is the proton rest energy. The data from the two flights are plotted in this form in Fig. 9. A proton spectrum of this form fits the experimental data well in the energy interval from 35 to 300 MeV with γ about 21 in the first flight and γ about 37 in the second. In the event of Sept. 3, 1960, this form also fits the data well in the entire energy interval from 30 to 600 MeV, as measured by rocket[20] and balloon borne[1] detectors. It is not possible to distinguish between a spectrum of the form given by Eq. (3) and the form given by Eq. (4) from the data of this work, since for $E/W_0 \ll 1$ Eq. (3) reduces to this form.

$$\ln(dN/dE)=\ln C-E/E_0, \tag{4}$$

where $E_0 = W_0/\gamma$.

─────────

[20] L. R. Davis, C. E. Fichtel, D. E. Guss, and K. W. Ogilvie, Phys. Rev. Letters **6**, 492 (1961).

Another feature of the proton energy spectrum is that at about 35 MeV, the slope abruptly changes to a large value as shown in Fig. 9. This feature is present in both flights. The data of Sept. 3, 1960, show a similar but less marked, change in slope. This abrupt change occurs at nearly the same energy in each case, although the slopes of the energy spectra above 35 MeV are very different.

As mentioned in Sec. III, a set of three hundred solar cosmic-ray particles was examined for the presence of isotopes of hydrogen other than protons. After elimination of fifteen helium particles, there remained 284 protons, one deuteron, and no tritons. A small number of secondary deuterons and tritons is produced in interactions of other particles in the air and are recorded in the emulsion while it is on the ground and during the ascent and descent of the detector through the atmosphere. In the area and solid angle scanned, the probability of finding a deuteron or triton from these sources is a few tenths. Therefore, the flux of deuterons and tritons in the solar particles is less than 1% of the protons in comparable energy intervals, and there is no positive evidence for any from our experiment.

B. He Nuclei

The differential energy spectra of solar He nuclei measured in the two flights are shown in Figs. 10 and 11 and Table IV. In the first flight the flux of solar particles in the energy range from 37.5 to 130 MeV/nucleon
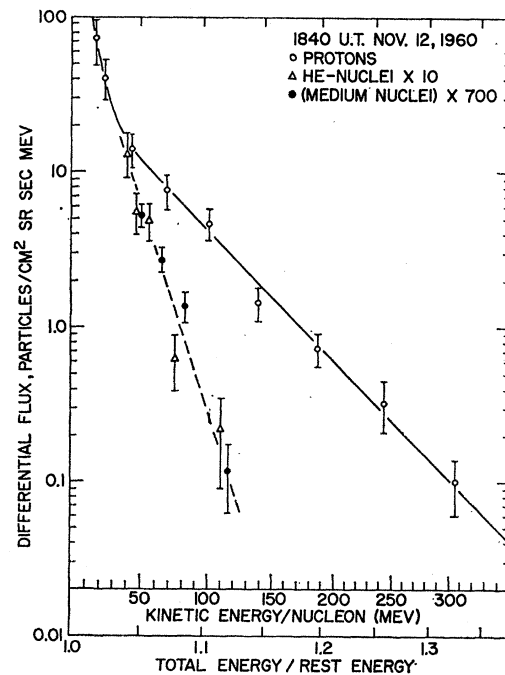

FIG. 10. Differential spectra for protons, He nuclei, and medium nuclei as a function of the total energy per nucleon in units of nucleon rest energy at 1840 U.T. Nov. 12, 1960. Note that the abscissa is an expanded logarithmic scale.

TABLE IV. Differential flux of He nuclei.

Kinetic energy interval (MeV/nucleon)	Flux in the interval (particles/ cm² sr sec)	Differential flux (particles/ cm² sr sec MeV)
(a) At 1840 U.T., Nov. 12, 1960		
37.7– 42.5	6.45	1.34 ±0.42
42.5– 50	4.18	0.56 ±0.16
50 – 60	4.85	0.49 ±0.13
60 – 90	1.92	0.064±0.026
90 –130	0.89	0.022±0.013
(b) At 1603 U.T. Nov. 13, 1960		
29.0– 32.5	19.53	5.58±1.68
32.5– 35.5	10.98	3.66±1.06
35.5– 41.5	10.80	1.80±0.52
41.5– 47.5	9.06	1.51±0.48
47.5– 57.5	9.90	0.99±0.30
57.5– 67.5	6.10	0.61±0.23
67.5– 95	4.24	0.15±0.07
95 –130	1.77	0.05±0.035

was 18.3±2.8 particles/(cm² sr sec). In the second flight on Nov. 13, a still higher flux of 41.4±6.2 particles/ (cm² sr sec) was seen in the same energy interval. From Fig. 10 and 11, it is seen that the spectra can be expressed in the form of Eq. (3). The value of γ was 63±7 in the first flight and 68±7 in the second flight.
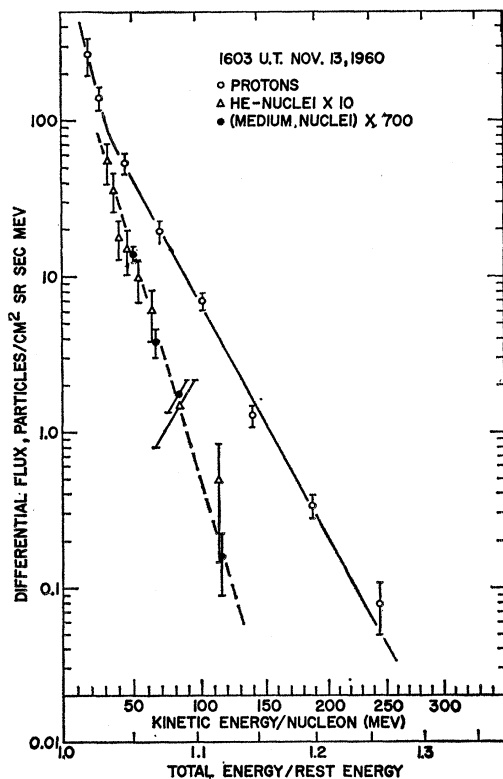

FIG. 11. Differential spectra for protons, He nuclei, and medium nuclei as a function of the total energy per nucleon in units of nucleon rest energy at 1603 U.T. Nov. 13, 1960. Note that the abscissa is an expanded logarithmic scale.
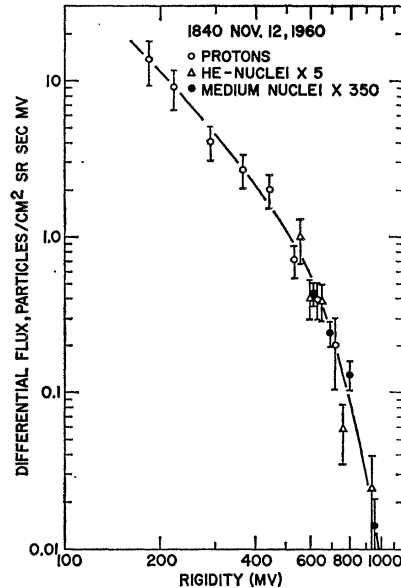

FIG. 12. Differential spectra of protons, He nuclei, and medium nuclei as a function of rigidity at 1840 U.T. Nov. 12, 1960.

Ney and Stein[2] measured solar He nuclei from this flare in balloon flights from Minneapolis at about 1900 U.T. on Nov. 13. Because this balloon flight was only about 3 h after the second rocket flight and the helium flux presumably did not change appreciably, we may compare the two results. Their differential He flux of 0.02±0.003 and 0.009±0.0015 particles/(cm² sec sr MeV) at 100 and 112 MeV/nucleon, respectively, agrees well with our results shown in Fig. 11.

C. Heavy Nuclei

Having obtained the flux and energy/nucleon spectra of the heavy nuclei, a large low energy component, energy/nucleon <300 MeV, was found in each of the flights, and a high-energy component, energy/nucleon >300 MeV, which was consistent with the normal cosmic-ray background. It has been shown previously[3] that the normal cosmic-ray flux of low-energy heavy nuclei is no more than a few particles/(m² sr sec) and can therefore be neglected. Hence, this large low-energy component represents the accelerated solar heavy nuclei.

The heavy particles which were included in the analysis, that is those whose emulsion equivalent range was greater than 1.7 mm, were found to be predominantly medium nuclei $(6 \leqslant Z \leqslant 9)$, rather than light nuclei $(3 \leqslant Z \leqslant 5)$, or large[21] nuclei $(Z \geqslant 10)$. Therefore, the discussion of the heavy nuclei will be begun by a treatment of the properties of the medium nuclei, since, in addition to being the most abundant heavy nuclei,

[21] The term "large nuclei" is introduced here to avoid the confusion which has arisen in the cosmic ray and astronomical literature resulting from "heavy" being used to refer to both nuclei with charges greater than two and those with charges greater than nine.
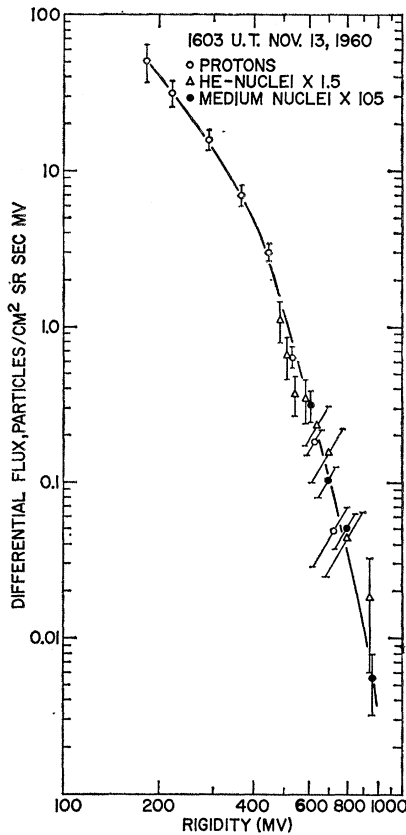
FIG. 13. Differential spectra of protons, He nuclei, and medium nuclei as a function of rigidity at 1603 U.T. Nov. 13, 1960.

TABLE V. Differential flux of medium nuclei.

Kinetic energy interval (MeV/nucleon)	Flux in the interval (particles/ m² sr sec)	Differential flux (particles/ m² sr sec MeV)
(a) At 1840 U.T. Nov. 12, 1960		
42.5– 54.9	969	78 ±13
54.9– 68.8	548	39.4± 7.4
68.8– 95	521	19.9± 4.5
95 –135	68	1.7± 0.8
(b) At 1603 U.T. Nov. 13, 1960		
42.5– 54.9	2463	198 ±24
54.9– 68.8	762	55 ±12
68.8– 95	663	25 ± 6
95 –135	91	2.3± 1.0

they also have nearly the same charge and the same charge-to-mass ratio.[22]

The differential energy per nucleon and rigidity spectra for medium nuclei are plotted in Fig. 10 and 11 for the flight at 1840 U.T., Nov. 12, and in Fig. 12 and 13 for the flight at 1603 U.T., Nov. 13, and are given in Table V. An extrapolation of the energy spectra to balloon altitudes would indicate that solar heavy nuclei even in this very large event are barely detectable at that level. This result explains why heavy nuclei have, in general, not been seen at balloon altitudes during solar cosmic-ray events in the past.

The other subject of interest in the study of the heavy nuclei is the charge spectrum, which is given in Table VI. Notice that within the medium group oxygen is somewhat more abundant than carbon, as spectroscopic evidence of the sun[23,24] indicates, and contrary to the situation in normal cosmic rays. The fact that

nitrogen is appreciably less abundant than carbon or oxygen is also in agreement with spectroscopic measurements of the sun.

The lack of any positive evidence for light nuclei and the relatively low limit set for their abundance is consistent with the relative abundance of this group in the sun, where they are less abundant than medium nuclei by a factor of 10^{-6} or more, and the very small amount of material the solar heavy nuclei have gone through. The ratio of light nuclei to medium nuclei in galactic cosmic rays at the top of the atmosphere is approximately 0.3 and is usually assumed to be essentially zero at the source.

There are small but measurable fluxes of the large nuclei; however, the abundance comparison to other species must be made at higher energies because the range of a nucleus for a given energy per nucleon, or velocity, is a decreasing function of the quantity Z^2/M. Neon is seen from Table VI to be 0.13±0.04 of the abundance of oxygen. There is no spectral evidence to indicate what the abundance of neon in the sun is; however, on the basis of stellar models, there is no reason to expect the abundance of neon relative to medium nuclei to be very different from the cosmic abundances,[25] where the neon to oxygen ratio is a few tenths. From Table VI it is seen that nuclei with a charge greater than ten were quite rare. The ratio of nuclei with charges $11 \leqslant Z \leqslant 18$ to oxygen nuclei in the same velocity interval is found to be 0.14±0.05 com-

TABLE VI. Charge spectrum of heavy nuclei in the same velocity interval with a base of 10 for oxygen.

Nuclear charge	4 and 5[a]	6	7	8	9	10	$11 \leq Z \leq 18$
1840 U.T. Nov. 12, 1960	<0.2	4.8±1.0	1.7±0.7	10	<0.3	1.4±0.5	1.1±0.7
1603 U.T. Nov. 13, 1960	<0.2	7.1±1.5	1.9±0.8	10	<0.3	1.2±0.5	1.6±0.7
Average	<0.2	6.0±0.9	1.8±0.5	10	<0.3	1.3±0.4	1.4±0.5

[a] Lithium ($Z=3$) is not included because the scanning efficiency for Li tracks was less than 100%. However, whenever Li occurs in nature, its abundance is similar to that of Be and B.

[22] Fluorine, of course, does have a slightly different ratio from the others, namely, 9:19 instead of 1:2 for the predominant isotope of each of the other three, but there is no positive evidence for fluorine amongst the solar particles, and it is relatively rare in general.

[23] L. Goldberg, E. A. Muller, and L. H. Aller, Astrophys. J. Suppl. 45, 1 (1960).

[24] L. H. Aller, The Abundance of the Elements (Interscience Publishers, Inc., New York, 1961).

[25] H. E. Suess and H. C. Urey, Revs. Modern Phys. 28, 53 (1956).

pared to the order of 0.09 given by spectroscopic evidence of the sun. The ratio of nuclei with $11 \leqslant Z \leqslant 18$ to medium nuclei in the solar cosmic rays of Nov. is 0.08 ± 0.03 compared to 0.25 ± 0.08 for galactic cosmic rays at the top of the atmosphere and 0.35 ± 0.10 for galactic cosmic rays extrapolated back to their source.[26]

There was one very large nucleus of low energy, probably in the iron group, but, since this could have been a cosmic-ray particle, no definite statement about detection of solar nuclei in this charge group can be made. If the nuclei in this group of very large charges occur in the same relatively small abundance as in the sun, their presence would not have been detected in the samples reported on here.

D. Comparison of H, He, and Medium Nuclei

Having obtained the flux and the energy spectra of solar protons, He nuclei, and medium nuclei, a comparison of these three components can be made. The differential energy spectra are plotted in Fig. 10 for the first flight and in Fig. 11 for the second flight. It is seen that the energy spectra of the He and medium nuclei have the same slope within uncertainties in both flights. On the other hand, the slope of the energy spectrum of the He nuclei, or medium nuclei, is much steeper than that of the proton component. Specifically γ, defined by Eq. (3) was 21 ± 2 for the proton component and 63 ± 7 for the multiply charged particles in the first flight, and the corresponding numbers for the second flight were 37 ± 2 and 68 ± 7.

TABLE VII. Relative abundances of protons, He nuclei, and medium nuclei.

Time	Proton Medium nuclei	Proton He nuclei	He nuclei Medium nuclei
42.5 MeV $\leqslant$ kinetic energy/nucleon $\leqslant$ 95 MeV			
1840 U.T. Nov. 12, 1960	2000±400	32±6	63±14
1603 U.T. Nov. 13, 1960	2650±430	36±7	72±16
Average Nov. 12, 13, 1960	2330±290	34±5	68±11
1408 U.T. Sept. 3, 1960	2650±790	32±10[a]	83±32[a]
1951 U.T. Nov. 16, 1960	1870±360[a]	26±7[a]	77±20[a]
570 MV $\leqslant$ rigidity $\leqslant$ 870 MV			
1840 U.T. Nov. 12, 1960	300±55	5 ±1	63±14
1603 U.T. Nov. 13, 1960	68±14	1 ±0.2	72±16
1408 U.T. Sept. 3, 1960	1100±380	13 ±5[a]	83±32[a]
1951 U.T. Nov. 16, 1960	105±35[a]	1.4±0.3[a]	77±20[a]

[a] Preliminary value, final value to be published later.

[26] See, for example, C. J. Waddington, *Progress in Nuclear Physics* (Butterworths-Springer, London, 1960), Vol. 8, and references listed therein.

TABLE VIII. Ratio of differential flux of protons to that of He nuclei as a function of kinetic energy per nucleon.[a]

Kin. energy MeV/nucleon	$\frac{dJ_p}{dE} \Big/ \frac{dJ_{He}}{dE}$				
	40	60	80	100	120
At 1840 U.T. Nov. 12, 1960	14	32	72	165	350
At 1603 U.T. Nov. 13, 1960	21	45	78	145	250

[a] These ratios are obtained from the best fitting lines for the differential spectra of protons and multiply charged nuclei. Since He nuclei and medium nuclei have the same energy spectra, the values for $(dJ_p/dE)/(dJ_m/dE)$ may be obtained by multiplying the above ratios by a factor of about 70. The error for the ratio at the lowest energy is about 30% and increases to about 50% at the highest energy.

In Figs. 12 and 13 the differential rigidity spectra of these three components are plotted for both flights. These figures show that the rigidity spectra of hydrogen, helium, and medium nuclei are similar; however, the proton data at the high rigidity end of the spectrum are of poor statistical weight and only extend up to about 800 MV as compared to 1000 MV for the multiply charged particles.

In Table VII, the relative abundances of protons, He nuclei, and medium nuclei are listed for equal energy per nucleon intervals and equal rigidity intervals for the two flights. For comparison, the values obtained in the Sept. 3, 1960 event[3] and preliminary results for one firing in the Nov. 15, 1960 event[27] are also given. The relative abundances for the same energy per charge are intermediate between those for the same energy/nucleon and the same rigidity. The lower limit of 42.5 MeV/nucleon in Table VII was set by the material above the emulsion and the minimum length of track required to identify the medium nuclei. The upper limit of 95 MeV/nucleon was chosen because essentially all of the multiply charged particles observed had energies less than this value, and there were no proton data above the corresponding rigidity value. These limits in rigidity correspond to 570 MV and 870 MV, respectively, for helium and medium nuclei which have a charge-to-mass ratio, Z/M, of 0.5. The proton energies corresponding to 570 MV and 870 MV are 160 and 338 MeV, respectively.

Since the helium and medium nuclei have the same energy spectrum, the helium-to-medium ratio is not a function of energy. The helium-to-proton ratio, and also the medium-to-proton ratio, is, however, a function of energy since their energy spectra differ. The proton-to-helium ratio as a function of energy is shown in Table VIII for both flights.

In Table VII, it is shown that the proton-to-helium and the proton-to-medium nuclei ratios in the same rigidity interval both vary greatly from one flight to another. On the other hand, the proton-to-helium and

[27] S. Biswas, C. E. Fichtel, and D. E. Guss, American Geophysical Union Meeting, Washington, D. C., April 1962 (unpublished).

the proton-to-medium nuclei ratios in the same energy/nucleon intervals are seen to be nearly the same each time. Thus, there is the striking situation that, although the energy per nucleon spectra for protons and multiply charged particles are different, the relative abundance of protons with respect to the others remains remarkably constant in the energy interval examined.

V. DISCUSSION

Having obtained the relative abundances of the energetic nuclei reaching the earth in a major solar particle event and determined the energy spectra of the major components at two different times in the event, a number of old hypotheses can be re-examined and a few new ideas put forth.

A. Modulation and Diffusion

In this section the problem of the interplanetary history of the energetic solar particles will be reviewed with emphasis on those areas to which the results of this work are related. Since the particles that are seen at the earth have already been acted upon by both the acceleration phase at their source and the transit phase, wherein they are modulated by the interplanetary conditions, it is necessary to try to disentangle the two effects. It seems convenient to proceed from the observations back to the source; so the discussion will begin with the transit phase.

It has been shown by Parker[28] that particle diffusion must predominate over particle drift in the interplanetary space because of the associated time scales. Several diffusion models for solar cosmic-ray particles have been developed,[28-30] and, in general, the diffusion coefficient which determines the rate of diffusion depends both on the particle velocity and its rigidity. Parker suggests that below a proton energy of the order of 1 BeV (the corresponding rigidity is approximately 2 BV), the diffusion coefficient depends primarily on the velocity of the particle and not the rigidity, because in this rigidity interval the radius of gyration of the particle is less than the scale length of the disordering of the magnetic fields. If this latter proposition is correct, one would expect the ratio of the differential proton energy spectrum,[31] dJ_p/dE, to the differential helium energy per nucleon spectrum, dJ_{He}/dE, at a given energy per nucleon, E, to be independent of time in the event at energies included in our study.[32] Remember

---

[28] E. N. Parker (private communication of work to be published).

[29] E. N. Parker, Phys. Rev. **103**, 1518 (1956).

[30] J. A. Simpson, Nuovo cimento, Suppl. 10, **8**, 133 (1958).

[31] Writing the differential spectra as a function of energy per nucleon is, of course, equivalent to writing it as a function of velocity for purposes of comparison, since two nuclei with the same energy per nucleon have the same velocity.

[32] This conclusion should not necessarily be made for balloon altitude experiments where the particle rigidities are higher and consequently closer to what is only an order of magnitude limit for the rigidity.

that the medium nuclei energy per nucleon spectrum was the same as the helium one within uncertainties; so in this discussion either the medium nuclei or the helium nuclei could be compared to the proton component. The two exposures studied here occurred at very different times in the Nov. 12, 1960 event, about 5 h and 27 h from the flare's beginning and under probably very different interplanetary conditions.[4] They, therefore, provide a good test of this hypothesis concerning the diffusion coefficient. In spite of the facts that the differential energy spectrum is very different from one flight to the next for a given component, and the slope of the helium curve is different from that of the proton one at a given energy per nucleon, the ratio $(dJ_p/dE)/(dJ_{He}/dE)$ is found to be the same within uncertainties for the two flights for those energies where comparisons can be made as shown in Table VIII. On the other hand, the ratio $(dJ_p/dR)/(dJ_{He}/dR)$, where R is rigidity, is very different. This result and the fact that similar abundances are seen in the same velocity intervals for three events are then in agreement with the prediction that the velocity predominates over the rigidity in the diffusion coefficient in this low rigidity interval, at least in these three events.

The experimental result of the near constancy of the ratio $(dJ_p/dE)/(dJ_{He}/dE)$ from one flight to another for any given energy studied further suggests that the difference in the energy per nucleon spectra between the protons and the helium nuclei is not due to the transition phase, but rather to the acceleration phase. This conclusion will be examined further in the next section on the acceleration process.

A few additional remarks can be made about the diffusion process. The theories referred to at the beginning of this section indicate that both inside of the region through which the particles diffuse and outside of it, there is an increase of the particle flux at any given energy to a broad maximum and then a relatively slow decline. Further, the high-energy particles will diffuse out more quickly with the result that the energy spectrum steepens with time, more quickly early in the event than later, when the decay phase is reached at all energies under consideration. All of these features have been observed many times,[33,34] including the observations of this event. This event is different from some of the others in that there was most probably a moving shock wave, or magnetic bottle wall, from a previous event wherein diffusion is much slower than in the surrounding region, as already mentioned in Sec. II. Although this feature does not alter the general remarks made above, it adds sufficiently to the complexity and uncertainty of the interplanetary conditions so as to make an exact functional prediction of the change in the spectral slope extremely difficult, if not impossible.

---

[33] W. R. Webber, *Progress in Cosmic Ray Physics* (Interscience Publishers, Inc., New York, 1961), Vol. 6.

[34] J. R. Winckler, P. D. Bhavsar, A. J. Masely, and T. C. May, Phys. Rev. Letters **6**, 488 (1961).

We shall, therefore, be content with saying that the general change in spectral slope noted in Sec. IV and shown in Fig. 8 is not unexpected.

B. Acceleration

Parker[35] has shown that within the framework of the present understanding of plasma dynamics, all particle acceleration mechanisms occurring outside of the laboratory are reducible to the Fermi mechanism[36–38] which is based on random particle collisions with magnetic inhomogeneities. The Fermi mechanism is divided into two phases, injection and acceleration. We shall begin with the former.

In order for acceleration to be effective, the initial particle energy must be sufficiently high so that energy losses due to interactions with ions and electrons are less than the energy gained by the Fermi process under the conditions existing in the medium. Parker[38] shows that in at least some regions the root mean square velocities may be such that the effective temperatures are 5×10^8 °K to 5×10^{10} °K, and the physical parameters are such that energy losses are completely negligible. Under these conditions, there is no problem of partial ionization, since an effective temperature of only 10^7 °K is needed to completely ionize oxygen.

Since the necessary injection energy is not the same for all nuclei, an unbiased sample of the sun will be obtained at the point of injection only if the root mean square velocity is much larger than the necessary injection velocity. In the model of Parker just mentioned, this condition is easily met for all nuclei being considered. No bias can occur in the proton-to-helium ratio from this cause alone because the necessary injection energy for protons and helium nuclei is the same.[39]

During the acceleration phase a Fermi type of process, in general, leads to an integral energy spectrum of the form

$$J(>W) = C_1/(W/W_0)^\alpha, \qquad (5)$$

or an equation that approaches this one in the low kinetic energy region. According to the calculation of Parker,[38] α of Eq. (5) is given by the expression

$$\alpha = 1/[4n_0(v/c)^2], \qquad (6)$$

where n_0 is the mean number of collisions before expulsion and v is the characteristic hydromagnetic velocity. Parker's actual equation differs from (5), but it can be shown to reduce to it for the case that $(E^2/2W_0W)$ is appreciably less than $1/\alpha$.

In the first order of the Fermi theory the energy spectrum of the particles does not depend on the charge nor mass of the particle, but only on the velocity as long as the particle is charged. The experimental results obtained here, together with the previous discussion on diffusion, however, show that the hydrogen nuclei have a flatter energy per nucleon spectrum, than the multiply charged particles; hence, 't is of interest to see how this might be explained. For a given velocity, the rigidity and, hence, the radius of curvature will be larger for the multiply-charged nuclei because of the larger mass-to-charge ratio. Therefore, the number of collisions before escape would in general be expected to be fewer both because a particle of higher rigidity is less likely to be reflected if the disturbed centers have random sizes, and because it is more likely to escape from the region. By Eq. (6) then, α would be larger for the helium and medium nuclei than for protons, as observed. From this point of view, the similar energy spectra for the helium and medium nuclei are a particularly strong argument for complete ionization.

In Sec. VA, it was noted that the diffusion process probably acts upon an initial spectrum in such a way as to yield a final spectrum which is related to the original one by a smoothly varying function of energy. It is not unreasonable then for an initial spectrum of the form given by Eq. (5) to be changed by the diffusion process in such a way as to yield a spectrum of the same form, but with a different value of α at different times in the event, as observed experimentally and shown in Figure 9.

Below 35 MeV there is a large additional group of low energy particles. Very large numbers of particles were seen at lower energies by Ogilvie et al.[12] in electronic instrumentation flown on the same flight, and also satellite data has, in general, shown relatively large proton fluxes in the 1.5- to 15-MeV region. These particles may be a sample of the original plasma from which the high energy particles were accelerated. Although the properties of these particles have probably been changed appreciably, a mean energy corresponding to the temperatures mentioned earlier, that is 0.05 MeV to 5 MeV seems reasonable on the basis of the relative number of particles at 1.5 MeV and the excess over the proposed Fermi component at 15 MeV.

If the above considerations are correct, there is some justification in extrapolating the proton, helium, and medium nuclei energy spectra to zero by means of a straight line on a graph of flux as a function of total

TABLE IX. Relative abundances deduced by extrapolation of integral fluxes to zero kinetic energy. (See Sec. VB for a discussion of this calculation.)

	Hydrogen/ helium[a]	Hydrogen/ medium nuclei[a]
1840 U.T. Nov. 12, 1960	16±5	$(1.0\pm0.3)\times10^3$
1603 U.T. Nov. 13, 1960	15±5	$(1.1\pm0.3)\times10^3$
Average	16±4	$(1.0\pm0.2)\times10^3$

[a] The errors include the uncertainty in the extrapolation process due to experimental uncertainties only, and do not include any attempt to evaluate this method of determining relative abundances.

[35] E. N. Parker, Phys. Rev. 109, 1328 (1958).
[36] E. Fermi, Phys. Rev. 75, 1169 (1949).
[37] E. Fermi, Astrophys. J. 119, 1 (1954).
[38] E. N. Parker, Phys. Rev. 107, 830 (1957).
[39] S. Hayakawa and K. Kitao, Progr. Theoret. Phys. (Kyoto) 16, 139 (1956).

energy per nucleon ignoring the additional low energy component below about 35 MeV, and then taking the extrapolated integral flux values at zero kinetic energy as representative of the relative abundances. Table IX gives the ratios thus obtained. Notice that the ratios are the same within errors in both flights and within the very wide limits set previously on the basis of spectroscopic evidence. The ratio thus obtained is certainly based on many assumptions and should be treated as such and not as a definite conclusion; however, we believe it is worth presenting because the ratios thus obtained do not involve the very uncertain ratios deduced by spectroscopic means. Relative abundances among the multiply charged components are, of course, unaltered and need not be repeated here.

C. Solar Cosmic Rays and the Sun

The detection of heavy nuclei in the Sept. 3, 1960 event,[3] in the Nov. 12, 1960 event, and also in the Nov. 15, 1960 event,[26] together with the fact that all present evidence points toward similar relative abundances in each case, indicates that the sun is capable of accelerating heavy ions to tens of MeV per nucleon or more and probably does so in every major solar event.

One of the questions of immediate interest then is whether or not the nuclei in solar cosmic rays reflect the relative abundances of elements comprising the sun's upper layers.

Leaving aside for a moment the problem of the proton having a different charge to mass ratio from that of essentially all of the other nuclei of interest by a factor of two, and hence a different velocity for a given rigidity, let us concentrate only on those nuclei with a charge of two or more. In the preceding sections, it was shown that there were good theoretical reasons for expecting the composition of the multiply charged component after the acceleration phase to reflect that of the sun, when the accelerated particle fluxes of the various nuclear components are compared in the same velocity intervals.

Once accelerated, the nuclei should behave similarly because the drift and diffusion mechanisms treat all nuclei with the same Z/M factor in the same way and the amount of material traversed in reaching the earth is certainly insignificant in terms of appreciably reducing the energy of even a 10 MeV per nucleon particle.

There is also some experimental evidence to indicate that a relatively unbiased sample of the multiply charged component of the sun has been obtained. The fact that not only were the relative abundances the same within uncertainties in three events, two of which were in completely different regions of the sun, but also at two different times in the same event suggests that charges are neither favorably accelerated nor discriminated against by the acceleration process. This hypothesis is strengthened by the fact that the relative abundances obtained in this experiment are consistent with

those obtained from spectroscopic measurements for those nuclei were determinations can be made by this latter method, namely, carbon, nitrogen, oxygen, and some of the larger nuclei. Good additional evidence is provided by the similar energy spectra for helium and medium nuclei.

If the ratios obtained here are accepted as representative of the sun, an estimate can be made of the abundance of elements, such as helium and neon, which cannot be determined with any reliability spectroscopically because they do not emit radiation, at least not strongly, in the optical range at normal solar temperatures. As stated earlier, the measured abundances of these two elements are both within expected limits. In addition, the carbon-to-oxygen ratio would now be determined with relatively fine precision, compared to the ratio obtained spectroscopically.

The next logical step is to attempt to determine the abundance of hydrogen with respect to some of the others, but especially helium. It has been stated previously that the protons might be expected to behave differently from the other nuclei and their different energy spectra confirmed this suspicion; so a ratio involving protons cannot be obtained simply. In order to circumvent the difficulty introduced by the different charge-to-mass ratios, the spectroscopic value of the hydrogen to medium nuclei ratio can be used. Unfortunately, there is considerable uncertainty in this value. A recent estimate based on a survey of available spectroscopic data[23,24] gave a hydrogen to medium ratio of 650, with an uncertainty probably of the order of a factor of 2. This number may then be combined with the solar helium to medium nuclei ratio obtained in this work to deduce a hydrogen to helium ratio of 10_{-5}^{+9}. Another approach to determining this ratio, which is based only on the interpretation of the solar cosmic-ray data, was discussed at the end of the preceding section on acceleration. It gave a hydrogen to helium ratio of 16 ± 4.

D. Comparison to Galactic Cosmic Rays

The information obtained on energetic solar particles can now be compared to the properties of galactic cosmic rays with the aim of seeing whether or not these solar particles and ones like them from other stars can be the source of ordinary galactic cosmic rays. Until a few years ago it was generally accepted that most stars could not be important sources of cosmic rays for a number of reasons. Within the last several years it had been noted that, since the sun produced large quantities of particles whose energies were well above the injection energy needed for the Fermi theory to be operative in the galaxy,[36,37] it might be possible that ordinary stars[40] were an important source of cosmic

---

[40] Here the term "ordinary star" refers to the great majority of stars with normal cosmic abundances and specifically excludes the unusual ones such as nova and supernova which may be important cosmic-ray sources.

rays. Relatively generous estimates of particle production by the stars indicated that protons could be supplied at a rate sufficient to account for the ordinary cosmic rays and these particles could then be accelerated in the galaxy by the Fermi method. There remained the problem of the charge composition of cosmic rays being different from normal stellar abundances, but it was thought that there might possibly be favorable acceleration of the larger nuclei.

The results of this experiment on the multiply charged component show that their abundances are just a reflection of those in the sun. There are at least four important differences within this group between solar cosmic rays and ordinary cosmic rays. Two of these, the carbon-to-oxygen ratio of $\frac{3}{5}$ in solar cosmic rays compared to $\frac{3}{2}$ in ordinary cosmic rays and the light-to-medium ratio of $<1/100$ in solar cosmic rays compared to $\frac{1}{4}$ in ordinary cosmic rays may be attributed to the fact that ordinary cosmic rays have gone through a few g/cm^2 of material wherein the light nuclei are formed by fragmentation, and there is at least an increase in the carbon-to-oxygen ratio. The other two, the different helium-to-medium nuclei ratios and the different ratios between the medium nuclei and those in the charge group with $11 \leqslant Z \leqslant 18$ are only enhanced by fragmentation. The helium-to-medium nuclei ratio is about five times larger for the accelerated solar particles, about 68:1 as compared to 14:1 for ordinary cosmic rays, and the ratio of the medium nuclei to those in the charge group with $11 \leq Z \leq 18$ was shown in Sec. IV C to be four times larger for the energetic solar particles.

At galactic cosmic-ray injection energies, the proton-to-medium ratio in solar cosmic rays is seen to be approximately 1×10^3 or larger. The proton-to-medium ratio for ordinary cosmic rays is about 250 for the same energy per nucleon intervals at very high energies and 100 for the same rigidity intervals. Thus, the proton-to-medium ratio for solar cosmic rays is 4 to 10 times the ordinary cosmic-ray ratio and the difference would be slightly increased by fragmentation in interstellar matter.

Thus, since the sun has abundances typical of most ordinary stars[40] in the respects mentioned here and since these abundances are reflected in solar cosmic rays, it seems reasonable to conclude that the difference in the charge composition between galactic cosmic rays and ordinary stars now remains as an objection to ordinary stars being considered as the sole primary source of galactic cosmic rays.